ADVANCED MATERIALS
www.advmat.de

Voluntary-Opsonization-Enabled Precision Nanomedicines for Inflammation Treatment

Shuya Li, Min Li, Shaohu Huo, Qin Wang, Jing Chen, Shenggang Ding, Zhutian Zeng, Wenchao Zhou, Yucai Wang, and Jun Wang**

Nanomedicines that target specific blood cells represent an emerging strategy to improve drug biodistribution. However, the protein corona usually disrupts nanomedicine targeting to cells and tissues. Herein, instead of exploring synthetic methods to mitigate the impact of the protein corona, its natural interactions with blood cells are leveraged and turn the protein corona into an active ingredient in treating lung inflammation. It is discovered that molecularly engineered liposomes with inverse phosphocholine lipids rapidly enrich complement fragment iC3b by "voluntary opsonization," which triggers neutrophil hijacking through complement receptor 3 phagocytosis. This neutrophil targeting is cell-state dependent as only those activated by acute inflammation display efficient neutrophil reconstruction. The liposome-loaded neutrophils migrate across the alveolar-capillary barrier, accumulate in the inflamed lung parenchyma within hours, and release their payloads to kill the bacteria. This work shows that, in addition to biological cells, the protein corona can be a new platform for active and precision nanomedicine.

In situ hitchhiking of blood cells as vehicles for nano-sized therapeutic and diagnostic agents is a promising strategy for drug delivery.[1] The privilege of these strategies has resulted from the innate delivery abilities of live cells such as circulation throughout the body, active crossing through biological barriers, and chemotactic homing to disease sites.[2] As the prerequisite for a successful hitchhiking, the nanomedicines should acquire a high binding affinity to desired cell types or populations. The general strategy for nanomedicines to hitchhike cells is to modify the surface of nanoparticles with antibodies or ligands that bind specifically to the receptors expressed on the target cell membranes.[3] However, the desired nanoparticle-cell interaction will be essentially blocked by the newly formed "protein corona."[4] Hence, the reliability and efficiency of hitchhiking desired cell subsets as a drug delivery strategy remains a fundamental challenge.

Once administrated intravenously (i.v.), the surface of nanomaterials is immediately covered by a layer of blood proteins, termed as the protein corona or biomolecular corona.[5] The amount and type of protein corona vary considerably in accordance with inherent physicochemical characteristics of nanoparticles, which inevitably alter the nano-biological interfaces such as targeting efficiency, immunogenicity, and intracellular toxicity of the particles.[6] Anti-fouling coating of nanoparticles such as poly(ethylene glycol) decoration was initially used to decrease the complications caused by the protein corona and to avoid the clearance by the mononuclear phagocyte system (MPS).[7] Recent studies have revealed that the purposeful adsorption of certain types of proteins, especially dysopsonins, could remodel the identity of nanomaterials. For instance, coating nanoparticles with albumin, clusterin in vivo, or pre-adsorption of apolipoprotein E in vitro prevented nonspecific uptake by phagocytic

Dr. S. Li, Dr. M. Li, Q. Wang, Dr. J. Chen, Prof. Z. Zeng, Prof. Y. Wang
Division of Molecular Medicine
Hefei National Laboratory for Physical Sciences at Microscale
the CAS Key Laboratory of Innate Immunity and Chronic Disease
School of Life Sciences
University of Science and Technology of China
Hefei 230027, P. R. China
E-mail: yucaiwang@ustc.edu.cn

S. Huo, Prof. S. Ding
Department of Pediatrics
the First Affiliated Hospital of Anhui Medical University
Hefei 230022, P. R. China

Prof. W. Zhou
Intelligent Pathology Institute
the First Affiliated Hospital of USTC
Division of Life Sciences and Medicine
University of Science and Technology of China
Hefei 230001, P. R. China

Prof. J. Wang
Institutes for Life Sciences, School of Biomedical Sciences and Engineering
National Engineering Research Center for Tissue Restoration and Reconstruction
Key Laboratory of Biomedical Engineering of Guangdong Province
South China University of Technology
Guangdong 510006, P. R. China
E-mail: mcjwang@scut.edu.cn

Prof. J. Wang
Bioland Laboratory (Guangzhou Regenerative Medicine and Health Guangdong Laboratory)
Guangzhou 510005, P. R. China

The ORCID identification number(s) for the author(s) of this article can be found under https://doi.org/10.1002/adma.202006160.

DOI: 10.1002/adma.202006160

cells and improved their circulation in blood.[8] Instead of trying to develop new methods to avoid its formation, we propose an unusual strategy, that is, by finely tuning the chemical composition of nanoparticles, we may engineer the protein corona with spontaneous enrichment of particular blood proteins. Such recruited proteins would have high affinity to certain blood cells to enable effective hitchhiking of the cells for nanoparticle transportation.

Herein, as a proof-of-concept, we demonstrate "voluntary opsonization" with naturally occurring complement fragments on nanoparticles to mediate selective targeting of activated neutrophils, the most abundant leukocytes are chemoattracted to inflamed sites (**Figure 1**A). The complement system is the first line of defense against foreign intruders by rapidly tagging and lysing them.[9] However, more interestingly, some pathogens take advantage of complement system to hitchhike cells through complement fragment iC3b "voluntary opsonization" and complement receptor 3 phagocytosis, which is also a safety mechanism for clearing apoptotic cells in vivo.[10] We demonstrate that liposomes composed of inverse phosphocholine lipids (CP) efficiently target activated neutrophils rather than the quiescent neutrophils, which are delivered to inflamed sites in the lung through neutrophil recruitment cascade. The complement fragment iC3b opsonization is responsible for the specific neutrophil entry by liposomes, as demonstrated by C3 binding and the receptor blocking assays. Neutrophils carrying liposomes migrate across the alveolar-capillary barrier into inflamed tissues, wherein neutrophils either release drug-loaded liposomes via the formation of neutrophil extracellular traps (NETs) or serve as micro-containers to confine both drug-loaded liposomes and bacteria intracellularly for bacteria killing, resulting in infection control (Figure 1B,C). This work suggests a new approach for precision nanomedicine, in which naturally occurring blood proteins are recruited to establish engineered protein corona for targeted drug delivery.

Initially, we prepared liposomes with varied surface physicochemical properties by changing the head-groups of the corresponding lipids. Specifically, the lipids had different head-groups and net charges but identical tails, which included anionic DOPG lipid, cationic DOTAP lipid, phosphocholine lipid of neutral DOPC, as well as inverse phosphocholine lipids of neutral DOCPe and anionic DOCP lipids (**Figure 2**A). The liposomes were prepared by a conventional thin-film hydration and extrusion method and hereafter denoted as n-DOPGs, n-DOTAPs, n-DOPCs, n-DOCPes, and n-DOCPs, respectively. Dynamic light scattering (DLS) measurement and cryo-transmission electron microscopy (cryo-TEM) observation revealed that the liposomes had a spherical morphology with an average size of ≈120 nm (Figure 2B; Figure S1, Supporting Information). Zeta potential measurements confirmed the different surface charges of the liposomes (Figure 2B).

To investigate the interactions of liposomes with circulating leukocytes in a mouse model of endotoxin-induced acute lung injury (ALI), which is characterized by a high fatality rate and extensive infiltration of neutrophils in lungs.[11] At 4 h post intranasal (i.n.) administration of lipopolysaccharide (LPS), we observed a ≈5-fold increase of neutrophils ($CD11b^{+}Gr\text{-}1^{high}$) (from 10.8 ± 1.5% to 50.0 ± 6.8% relative to total leukocytes) in blood (Figure S2, Supporting Information). The upregulation of CD11b expression on neutrophils was observed after LPS administration, indicating the rapid activation of neutrophils (Figure S3, Supporting Information).[12] The ALI mice were further i.v. administrated with liposomes labeled with fluorescent dye 3,3′-dioctadecyloxacarbocyanine (i.e., n-DOPCs@DiO, n-DOCPes@DiO, n-DOCPs@DiO, n-DOPGs@DiO, n-DOTAPs@DiO). At 10 min post administration, the ALI mice showed a 10.3-fold increase in the ratio of n-DOCPs@DiO^{+} neutrophils ($CD11b^{+}$ $Gr\text{-}1^{high}$, Figure S4, Supporting Information) and a 21.1-fold increase in cellular n-DOCPs@DiO mean fluorescence intensities (MFI) of neutrophils in blood compared to healthy mice (i.e., without *i.n.* LPS administration) (Figure 2C). This observation confirmed that n-DOCPs were able to selectively tag to inflammation-activated circulating neutrophils, rather than the resting ones. By contrast, the internalization of n-DOPCs@DiO and n-DOCPes@DiO by neutrophils was minor due to their intrinsic anti-fouling properties of the zwitterionic head-groups,[13] and the internalization of other charged liposomes by neutrophils were lower than n-DOCPs. We further quantitatively compared the distribution of liposomes among various leukocyte subsets by multiplying the percentage of individual leukocyte population with their cellular MFI of DiO (Figure 2D). In the ALI model, approximately 70.4% of n-DOCPs in blood were encapsulated in activated neutrophils (Figure 2D).

To observe the dynamic interactions between n-DOCPs and activated neutrophils, we imaged the vessels in the inflamed ear of mice induced by endotoxin. At 2 h post LPS challenge, the mice were injected with PE-labeled Ly6G antibody and 1,1′-dioctadecyl-3,3,3′,3′-tetramethylindotricarbocyanine perchlorate (DiD)-labeled n-DOCPs (n-DOCPs@DiD) or n-DOPCs (n-DOPCs@DiD, as an anti-fouling and long circulating control). Immediately, the blood vessels under the ear skin were imaged using intravital microscopy (IVM). The majority of neutrophils in LPS-challenged mice appeared to be elongated and were adherent to or slowly crawling along the endothelium, all of which were the prototypical features of activated neutrophils. These cells were rapidly targeted by n-DOCPs within 6 min (Figure 2E; Movie S1, Supporting Information). By contrast, the long blood circulating n-DOPCs freely flowed through the vessels without co-localizing with activated neutrophils, leaving behind some dark areas in places where the neutrophils occupied (Figure 2F; Movie S2, Supporting Information). Moreover, high-resolution imaging of neutrophils isolated from blood revealed the accumulation of n-DOCPs but not n-DOPCs in the cytosol of activated cells (Figure S5, Supporting Information).

To explore the mechanisms underlying the targetability of n-DOCPs to activated neutrophils, we examined two essential determinants, including: 1) the functional state of neutrophils and 2) the protein corona adsorbed on n-DOCPs. Activated and resting neutrophils were respectively isolated from bone marrows of mice with and without intraperitoneal (i.p.) LPS administration, and the activation of neutrophils was evidenced by the elevated expression of CD11b (**Figure 3**A; Figure S6, Supporting Information). To mimic the formation of protein corona under the in vivo inflammatory conditions, we used plasma or serum from LPS-challenged mice for the co-incubation of DiO-labeled liposomes and neutrophils. After 1 h incubation in the presence of plasma, activated neutrophils internalized

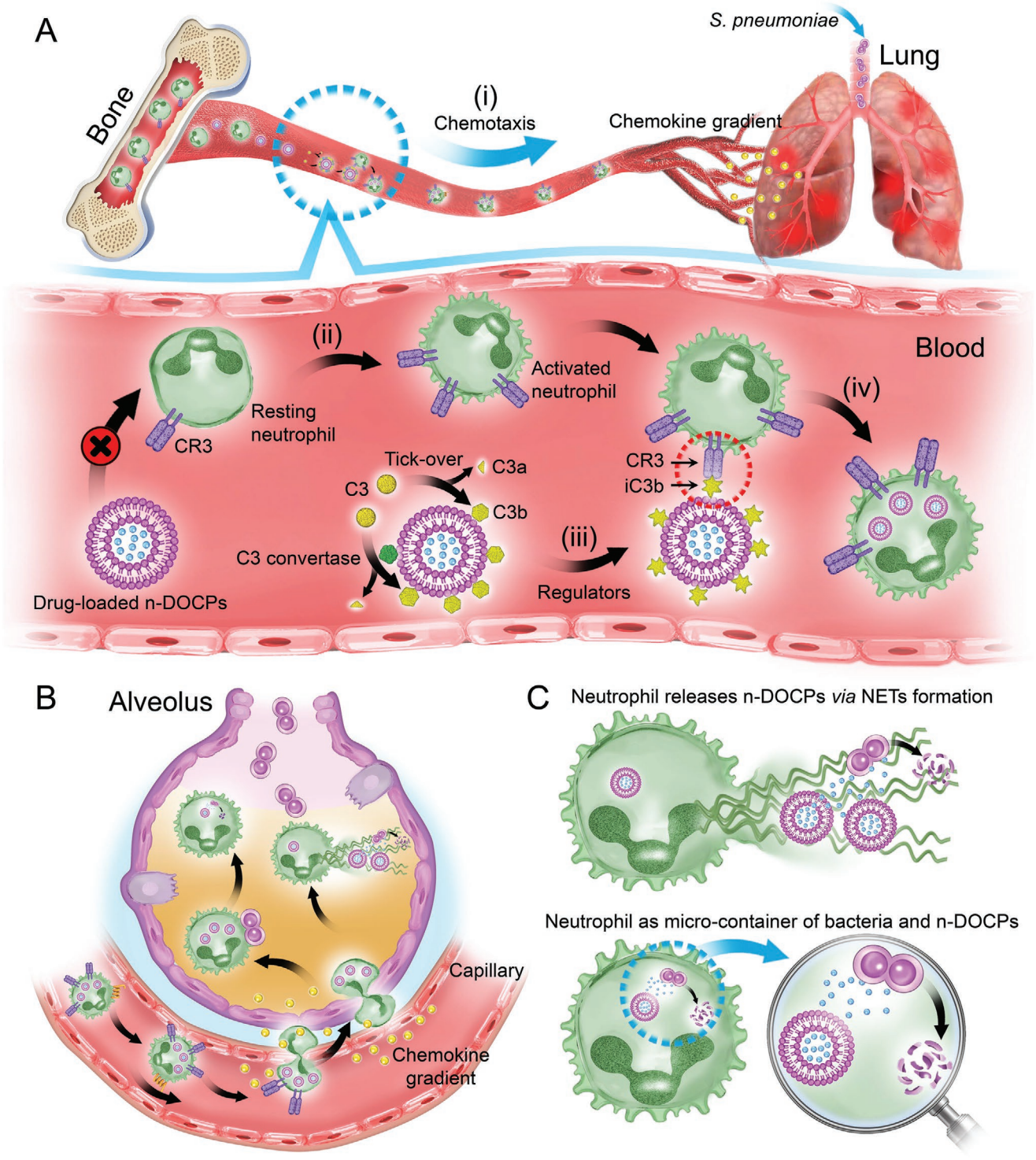

Figure 1. Schematic showing the concept of complement fragments tagging on the nanoparticles mediated rapid neutrophilic entry for inflammation targeting. A) i) Chemokine gradient produced in response to acute lung inflammation induced by intranasal (i.n.) administration of *S. pneumoniae*. ii) Neutrophils are activated in the inflammation condition and upregulated the expression of complement receptor 3 (CR3). iii) Complement protein C3 is cleaved by tick-over or C3 convertase to generate activated fragment C3b, which quickly tags on n-DOCPs surface and is further degraded into iC3b by complement regulators. iv) The binding of iC3b to CR3 achieves the entry of n-DOCPs into activated neutrophils, rather than resting ones. B) Schematic showing that n-DOCPs-loaded neutrophils migrate across the alveolar-capillary barrier to inflamed alveoli in response to chemokine gradient. C) Two possible mechanisms involved in the bacteria-killing effect of n-DOCPs loaded neutrophils. On the one hand, neutrophils release encapsulated n-DOCPs through the formation of NETs. On the other hand, neutrophils serve as cellular microcontainers to intracellularly confine both n-DOCPs and the bacteria, enabling a high local concentration of antibiotics to kill bacteria.

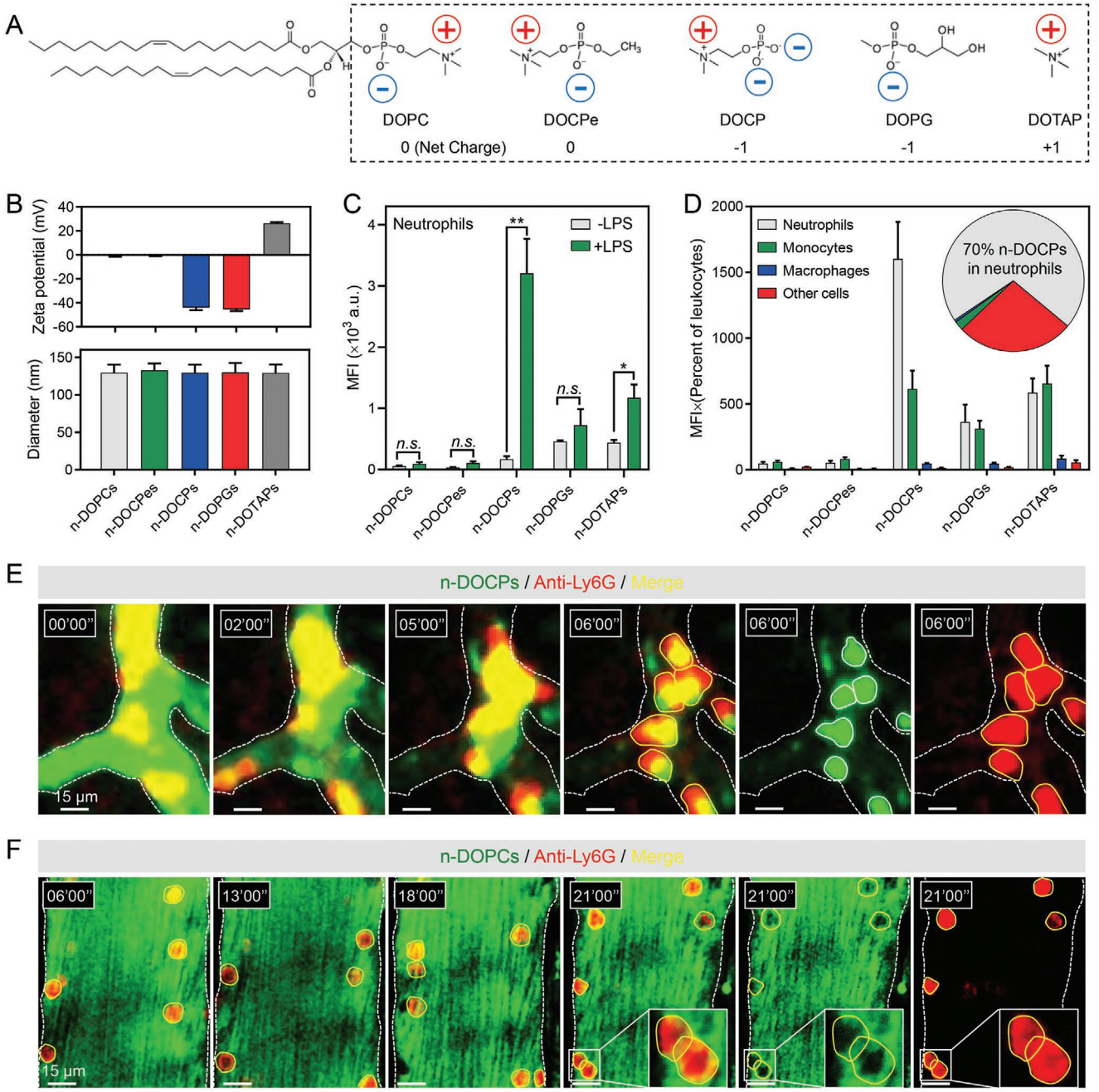

Figure 2. n-DOCPs targeted activated neutrophils in inflammatory mice, but not resting ones in healthy mice. A) Illustration of the chemical structure and net charge of DOPC, DOCPe, DOCP, DOPG, and DOTAP lipids. B) DLS measurements of the zeta-potential and the diameters of n-DOPCs, n-DOCPes, n-DOCPs, n-DOPGs, and n-DOTAPs. C) Flow cytometry analyses of cellular DiO MFI of neutrophils in peripheral blood of mice received DiO-labeled liposomes i.v. injection. $*p<0.05$, $**p<0.01$, n.s., not significant. D) Distribution of liposomes in different leukocytes in blood of mice with LPS stimulation as defined by multiplying the percentage of leukocytes with cellular MFI of DiO. The inset showed the relative distribution of n-DOCPs in the major phagocytes in blood as calculated using the equation $(\text{MFI}x \times \text{Percentage}x)/\Sigma(\text{MFI}x \times \text{Percentage}x)$, "$x$" represents neutrophils, monocytes, macrophages, or other cells. E) Real-time intravital microscopy of dynamics of n-DOCPs (green) and F) n-DOPCs (green) with neutrophils (red) in the mice ear vessel after subcutaneous injection of LPS. The white dotted curves and yellow solid curves indicated the vessel walls and neutrophils, respectively.

1.7-fold more n-DOCPs than the resting ones, confirming that the activation of neutrophils was the prerequisite of the specific targeting of n-DOCPs (Figure 3B). In contrast, the uptake of other liposomes was independent of the functional state of neutrophils. In the presence of serum, that is, plasma without fibrinogen that has been reported to inhibit complement activation,[14] activated neutrophils showed even higher ability of preying n-DOCPs than the resting ones (Figure S7, Supporting Information).

The high-expressed CD11b on activated neutrophils is the α chain of complement receptor 3 (CR3). CR3 is known to mediate neutrophil adhesion as well as phagocytosis.[15]

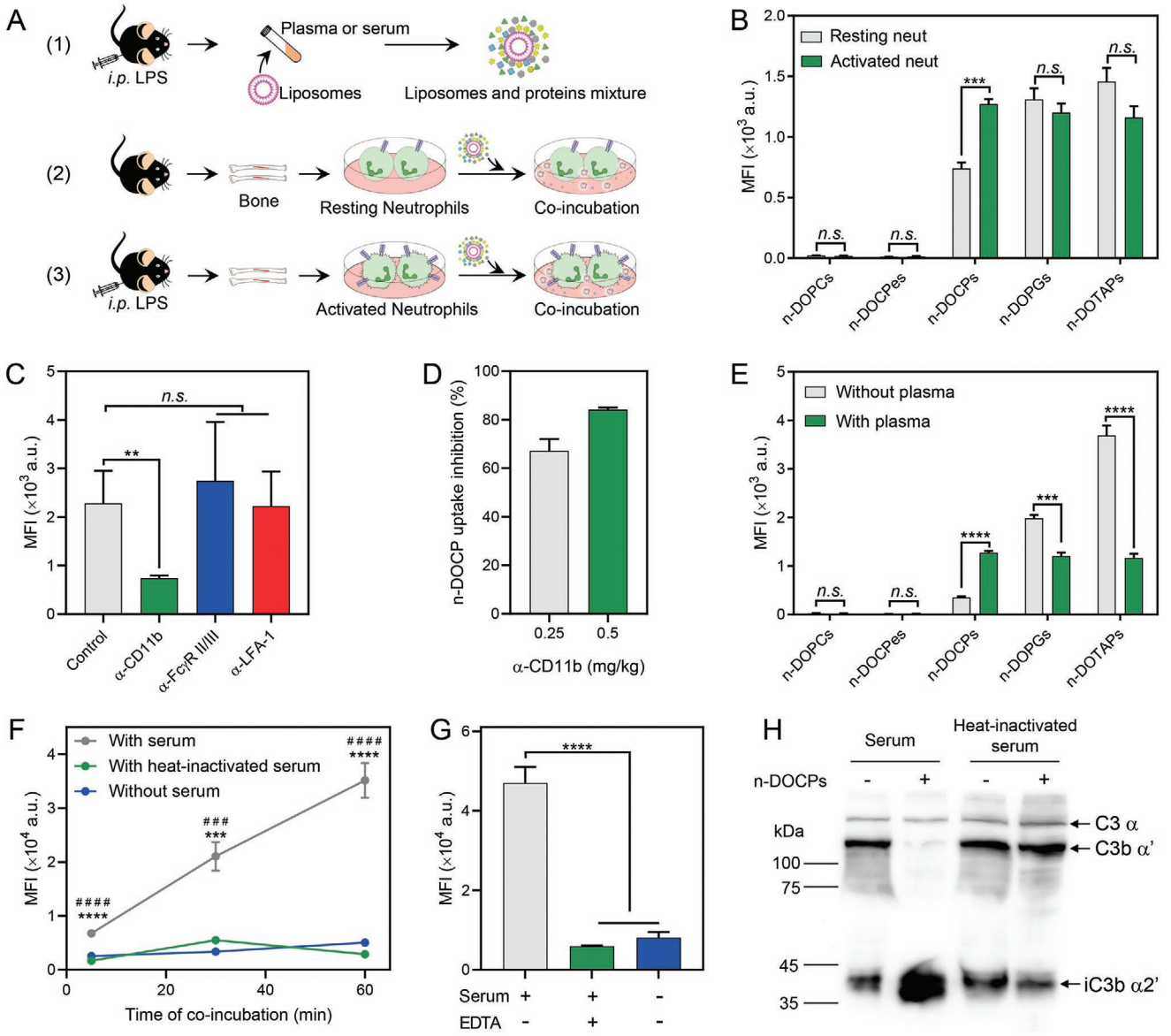

Figure 3. Complement proteins coating on n-DOCPs mediated rapid neutrophil targeting. A) The plasma and serum were collected from LPS-challenged mice. The DiO-labeled liposomes were mixed with plasma or serum. Activated and resting neutrophils were isolated from bone marrow of mice with and without (i.e., healthy mice) i.p. LPS administration, respectively, and incubated with liposomes in vitro. B) Cellular DiO MFI of resting and activated neutrophils after being incubated with DiO-labeled liposomes in the presence of plasma for 1 h. C) Cellular DiO MFI of activated neutrophils in peripheral blood of LPS-induced ALI mice. The mice were i.v. injected with the antibodies followed by n-DOCPs@DiO injection. D) The inhibition ratio of n-DOCPs uptake by neutrophils after CD11b receptor blocking. E) Cellular DiO MFI of activated neutrophils which were incubated with DiO-labeled liposomes in the presence or absence of plasma for 1 h. F) Time-dependent change of cellular DiO MFI of activated neutrophils that were incubated with n-DOCPs@DiO in the presence of either serum or heat-inactivated serum. ***$p<0.001$, ****$p<0.0001$ versus the heat-inactivated serum group. ###$p<0.001$, ####$p<0.0001$ versus the without serum group. G) Cellular DiO MFI of activated neutrophils which were incubated with n-DOCPs@DiO in the presence of either serum or the serum with EDTA. H) Gel electrophoresis and western blot analysis of C3 in the serum or in the protein corona of n-DOCPs. **$p<0.01$, ***$p<0.001$, ****$p<0.0001$, n.s., not significant.

We therefore sought to examine whether the internalization of n-DOCPs was mediated by the up-regulated CR3. Pre-treatment of inflammatory mice with CD11b antibody (α-CD11b) to block the CR3 significantly inhibited the uptake of n-DOCPs (Figure 3C). And we observed that the uptake of n-DOCPs by activated neutrophils was decreased by 67.2% ± 8.5% and 84.2% ± 1.5% after CR3 blockade using 0.25 and 0.5 mg kg^{-1} of α-CD11b, respectively (Figure 3D). Lymphocyte function-associated antigen-1 (LFA-1 or $\alpha_L\beta_2$ integrin) and Fcγ receptors (FcγRs) are also the primary surface receptors on neutrophils that can mediate adhesion and phagocytosis, respectively.[16] However, the blockade of these receptors by antibodies of α-LFA-1 and α-FcγR II/III, had no effect on the uptake of n-DOCPs by neutrophils (Figure 3C). Thereby, the internalization of n-DOCPs into activated neutrophils was mainly mediated by the upregulated complement receptor 3.

We next studied the role of protein corona in the neutrophil uptake of n-DOCPs. Without plasma or serum, the uptake of n-DOCPs by activated neutrophils decreased by 72.5% and 91.8% after 1 h co-incubation, respectively, suggesting that the specific neutrophil targeting was dependent on certain protein components adsorbed on the particles (Figure 3E,F). Interestingly, pre-incubation with plasma decreased the internalization of n-DOPGs and n-DOTAPs by neutrophils, probably because the direct interaction between charged nanoparticles and cell membrane was shielded after protein coating (Figure 3E). At the same time, the uptake of neutral liposomes (n-DOPCs or n-DOCPes) was not affected.

To determine the involvement of complement proteins, we heat-inactivated serum (56 °C, 30 min) since most of the proteins involved in the complement activation are heat-labile.[17] With the heat-inactivated serum, we observed marginal internalization of n-DOCPs by activated neutrophils similar to that without serum incubation (Figure 3F). Moreover, when complete inhibition of complement activation was achieved by chelation of divalent cations with 10 mM ethylenediaminetetraacetic acid (EDTA),[18] we observed the loss of the ability of the serum to promote the uptake of n-DOCPs by activated neutrophils, indicating the involvement of complement opsonization in the entry of n-DOCPs into activated neutrophils (Figure 3G). We next investigated the underlying mechanisms for complement opsonization of n-DOCPs. It has been reported that protein corona of nanoparticles, rather than the native nanoparticle surface, provide active sites for complement binding and amplification.[19] We used isothermal titration calorimetry (ITC) to assess the thermodynamic properties of the binding reactions between bovine serum albumin (BSA) and liposomes. The titration of BSA to n-DOCPs showed the highest heat release compared to other liposomes, indicating the strong binding affinity between them, which might be explained by the hydrogen and electrostatic interactions between phosphate groups on n-DOCPs surface and guanidine groups of arginine residue on BSA (Figures S8 and S9, Supporting Information).[20] Meanwhile, label-free quantitative liquid chromatography mass spectrometry was performed to analyze the proportion of C3, the central complement effector molecules, absorbed on liposomes. The results showed that the amount of adsorbed C3 of n-DOCPs (4.4%) was higher than that of n-DOPG (2.4%) and n-DOTAP (0.7%) (Figure S10, Supporting Information). Thus, we conclude that n-DOCPs provide a more stable protein corona for C3 fixation and amplification, which collectively lead to selective neutrophils targeting.

To further verify the presence of C3 on n-DOCPs, the protein coronas on n-DOCPs were separated with sodium dodecyl sulfate-polyacrylamide gel electrophoresis (SDS-PAGE) under reducing conditions and analyzed by western blot using recombinant anti-C3 monoclonal antibody. The results showed that almost all C3 fragments bound on n-DOCPs were degraded into iC3b with a much higher level than that in the serum (Figure 3H). However, there was no enrichment of iC3b on n-DOCPs after incubation with heat-inactivated serum, suggesting that the proteolytic cascade activation is required for the enrichment of iC3b on n-DOCPs. Given that the CR3 is recognized as the receptor for the complement fragment iC3b,[21] it is reasonable to conclude that the internalization of n-DOCPs by activated neutrophils is mainly mediated by iC3b-CR3 binding.

The alveolar-capillary barrier is formed by the capillary wall and alveolar wall. The barrier is mostly impermeable to most solutes and prevents fluid exchange between vasculature and alveoli (**Figure 4**A).[22] In endotoxin-induced mice ear inflammation model, we observed migration and transmigration of neutrophils containing n-DOCPs@DiD from blood into the deep tissue (Figure 4B; Movie S3, Supporting Information). To directly quantify the numbers of n-DOCPs@DiO^+ neutrophils in bronchoalveolar lavage fluid (BALF) using flow cytometry, we found the percentage of n-DOCPs@DiO^+ neutrophils showed a steep rise from 7.2% at 10 min post injection reaching to 96.2% at 30 min (Figure 4C). The enhancement occurred concurrently with the decrease of n-DOCPs@DiO^+ neutrophils in the blood (Figure S11, Supporting Information). With the same settings, there were less than 21.7% of n-DOPCs@DiO^+ neutrophils in BALF, ruling out the possible enhancement of tissue infiltration of n-DOCPs@DiO due to LPS-induced barrier disruption. Direct imaging of the major organs excised at 30 min post liposomes injection showed that the 53.1% of injected n-DOCPs were accumulated in the inflamed lungs, in contrast to 16.6% for n-DOPCs (Figure 4D). In addition, closer analyses of fluorescence ratios of lung to liver further demonstrated the remarkable targetability of n-DOCPs to the inflamed lung (Figure 4E).

To explore the potential of activated neutrophils to deliver nanomedicines to the lung and relieve ALI and bacterial infection, we first tested whether the n-DOCPs uptaken by neutrophils could be released at the inflamed sites. Leukocytes isolated from the BALF of n-DOCPs@DiD-treated ALI mice were stained with PE-labeled anti-Ly6G and DAPI. The plasma membranes of most neutrophils were disrupted, accompanied by the release of web-like DNA, indicating the formation of NETs (Figure 4F).[23] Thus, it is understandable that the n-DOCPs in neutrophils could be released under the inflammatory condition. Moreover, a mouse model of pneumococcal pneumonia was established by instilling clinically isolated *Streptococcus pneumoniae* (*S. pneumoniae*) into the mouse nostrils. As expected, the *S. pneumoniae* infection increased the proportion and number of neutrophils in blood and BALF (Figure S12, Supporting Information). One major challenge in the clinical use of antibiotics to treat *S. pneumoniae* infection is that bacteria can hide inside phagocytes to avoid antibiotic contact because of the antibiotics lacking cellular accumulation.[24] Interestingly, we observed that neutrophils in BALF simultaneously phagocytosed both n-DOCPs and *S. pneumoniae*, as evidenced by the co-localization of their fluorescence signals in the cytosol of neutrophils (Figure 4G). Thus, for n-DOCPs, neutrophils also served as cellular micro-containers that could confine both antibiotics and the bacteria intracellularly and hence enabled a high local concentration of antibiotics to kill bacteria.

For the evaluation of the ability of drug loaded n-DOCPs to relieve ALI, the mice pre-challenged with LPS were treated with a single i.v. injection of free dexamethasone (Dex), n-DOPCs@Dex, or n-DOCPs@Dex at an equivalent Dex dose of 5 mg kg^{-1}, respectively (**Figure 5**A). Free Dex and n-DOPCs@Dex treatments mildly reduced the level of inflammatory factors TNF-α and IL-6 in BALF and serum (Figure 5B,E). By contrast, n-DOCPs@Dex treatment achieved the maximum reduction of TNF-α and IL-6. After n-DOCPs@Dex therapy, a

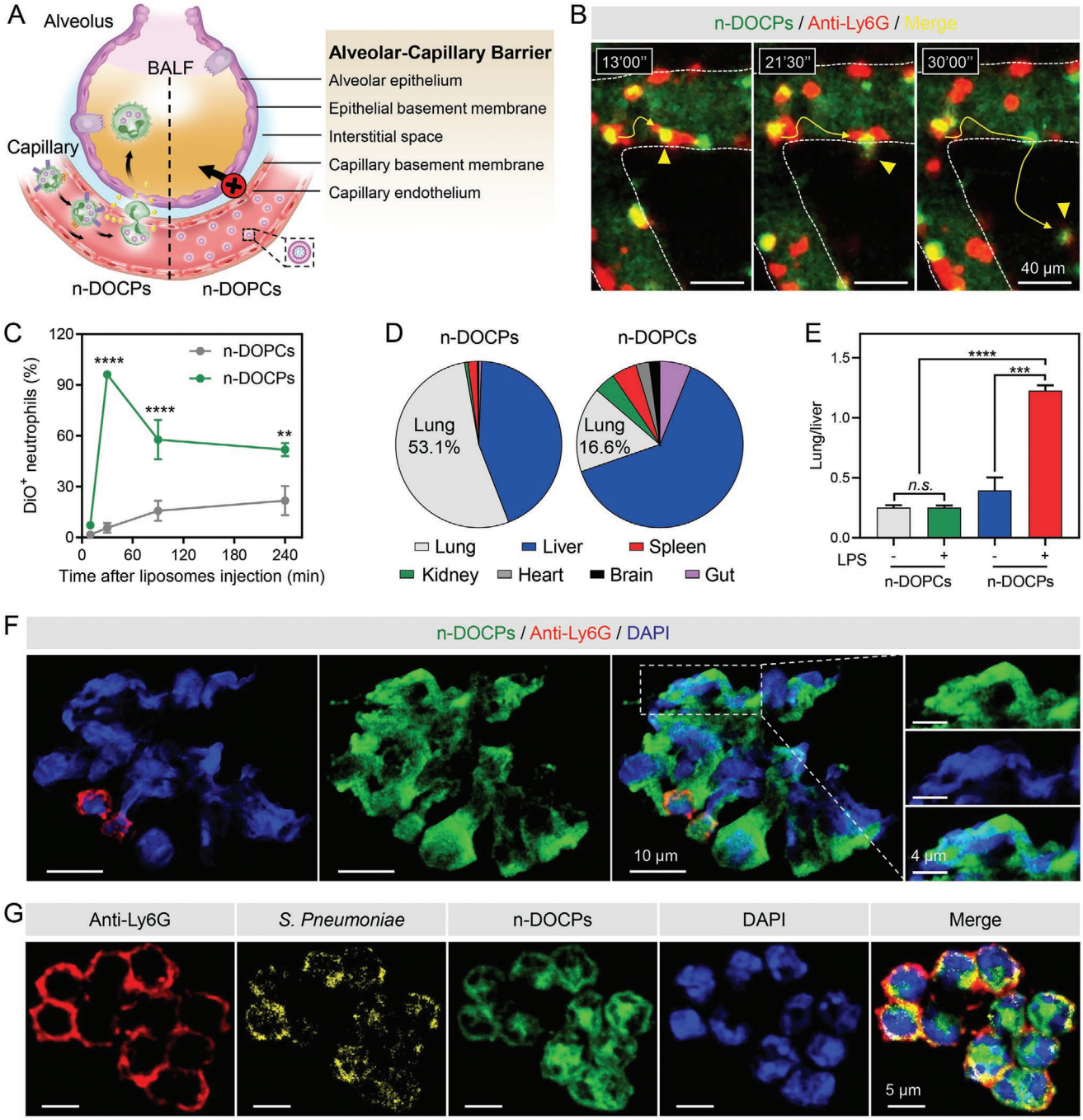

Figure 4. Activated neutrophils transported n-DOCPs to cross alveolar-capillary barrier and enabled its enrichment in inflamed lung. A) Schematic showing the active transport of n-DOCPs-loaded neutrophils across the alveolar-capillary barrier in response to chemokine gradient. By contrast, long-circulating n-DOPCs were trapped in the bloodstream. B) IVM imaging of inflamed blood vessels showed the migration and extravasation of neutrophils (red) laden with n-DOCPs (green). The white and yellow curves indicated the vessel walls and the motion paths of neutrophils, respectively. C) Time-dependent change of percentages of DiO^+ neutrophils in BALF of LPS challenged mice that received injection of n-DOCPs@DiO and n-DOPCs@DiO. D) The relative distribution of n-DOPCs and n-DOCPs in organs of inflammatory mice. E) The lung-to-liver accumulation ratio of n-DOCPs and n-DOPCs in mice challenged with and without LPS. F,G) Confocal microscopy observation of neutrophils (red) extracted from alveolus of LPS-stimulated (F) and *S. pneumoniae* (yellow)-infected (G) mice treated with n-DOCPs (green). Cell nuclei were stained with DAPI (blue). $^{**}p<0.01$, $^{***}p<0.001$, $^{****}p<0.0001$, n.s., not significant.

significantly lower number of infiltrated neutrophils in the inflamed lung was observed (Figure 5F; Figure S13, Supporting Information, 0.9×10^3 neutrophils mm^{-2} compared to 2.5×10^3 neutrophils mm^{-2} for control). In addition, haematoxylin and eosin (H&E) staining showed that mice receiving LPS stimulation exhibited severe lung injury and pulmonary

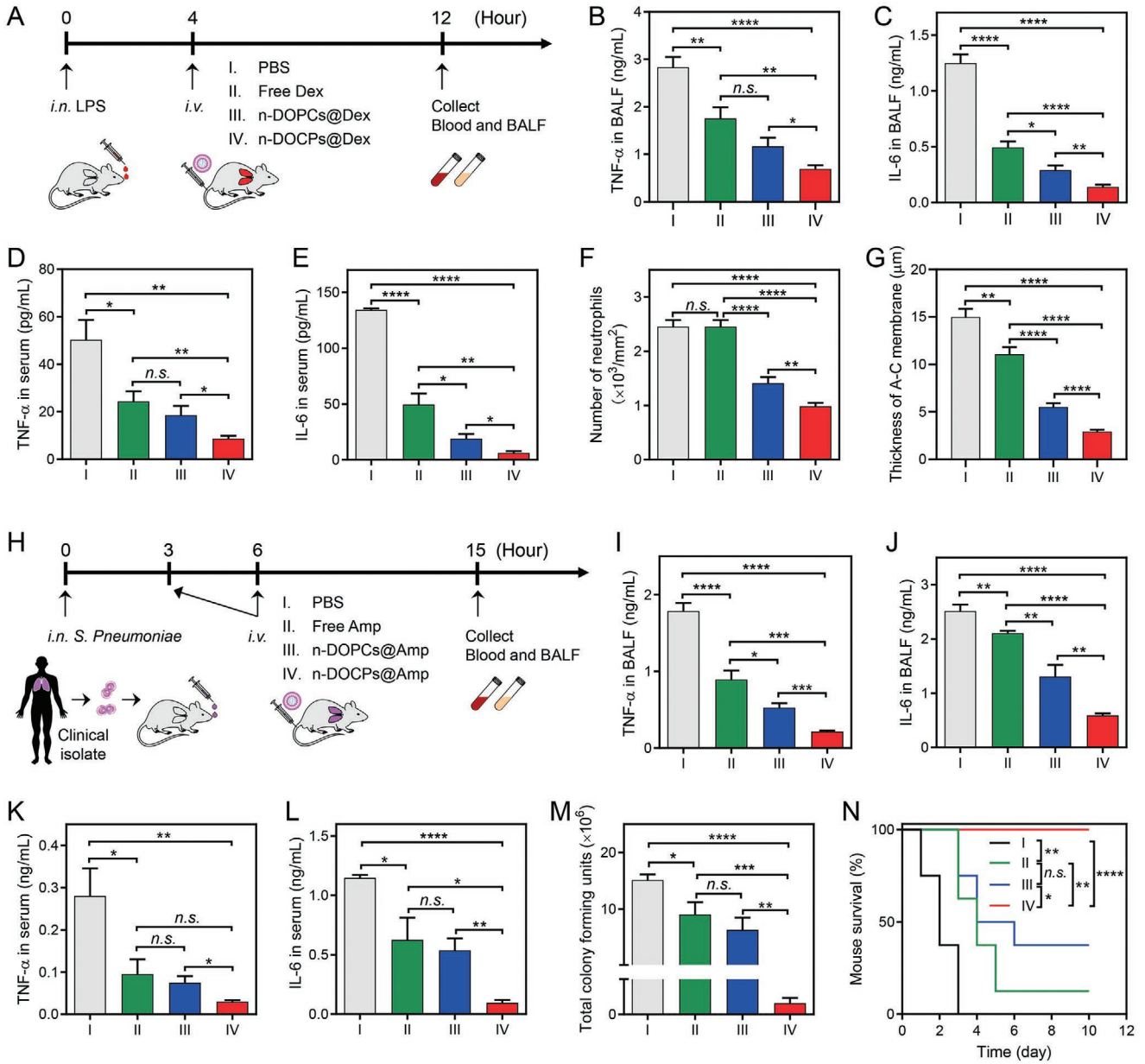

Figure 5. Neutrophils-mediated delivery of drug-loaded n-DOCPs mitigated acute lung injury and pneumococcal pneumonia. A) Schedule for the experiments in (B) to (E). B–E) Concentrations of TNF-α and IL-6 in BALF (B,C) and in serum (D,E). F) Quantitative analyses of neutrophils in the lung tissues at 24 h after therapy. G) Quantitative analyses of the thickness of alveolar-capillary membrane (A-C membrane) in the lung tissues at 24 h after therapy. H) Schedule for the experiments in (I) to (M). I–L) Concentrations of TNF-α and IL-6 in BALF (I,J) and in serum (K,L). M) Total colony forming units of *S. pneumoniae* in BALF. N) Kaplan–Meier survival curve of mice infected with high dose of *S. pneumoniae*. *$p<0.05$, **$p<0.01$, ***$p<0.001$, ****$p<0.0001$, n.s., not significant.

fibrosis, as evidenced by the thickening of the alveolar-capillary membrane and massive cell infiltration. Treatment with n-DOCPs@Dex efficiently prevented alveolar fibrosis and attenuated such pathological changes (Figure 5G; Figure S14, Supporting Information).

Encouraged by the above observations, we further used ampicillin (Amp), a broad-spectrum antibiotic, to explore the therapeutic outcomes of Amp-loaded n-DOCPs (n-DOCPs@Amp) against pneumococcal pneumonia. The mice were i.v. treated with free Amp, n-DOPCs@Amp, and n-DOCPs@Amp at 3 and 6 h after infection, respectively (Figure 5H). n-DOCPs@Amp dramatically attenuated the lung inflammation, as evidenced by the significant drops of inflammatory cytokines TNF-α and IL-6 in both BALF and serum (Figure 5I,L). Direct quantification of *S. pneumoniae* in BALF using a bacterial plate count method also revealed a 99.7% inhibitory efficacy on the bacterial growth in BALF for n-DOCPs@Amp relative to control groups (Figure 5M). In addition, the high-dose *S. pneumoniae* inoculation (2×10^9 CFU/mouse) caused 100% death in control group within 72 h (Figure 5N), while n-DOPCs@Amp and free

Amp treatments could moderately improve the mouse survival. By contrast, n-DOCPs@Amp treatment cured all the mice with no deaths being observed.

In summary, we developed liposomes composed of CP lipids, which can efficiently target activated neutrophils through the specific interaction between cell-bound complement receptor CR3 and adsorbed complement fragments iC3b in vivo. Under inflammatory stimulation, this "voluntary opsonization" process bestows particle with outstanding targetability and motility. The chemotaxis of activated neutrophils overcomes the obstacles encountered by free nanoparticles and dramatically enhances the accumulation of particles inside the inflamed lung area. Then neutrophils can either act as micro-containers or release n-DOCPs in response to inflammatory stimuli to kill bacteria, achieving remarkable therapeutic efficacy. Collectively, the strategy of utilizing the protein corona on nanoparticles during administration to target circulating cells for enhanced nanomedicines delivery could bring new opportunities in the development of a novel drug delivery system.

Experimental Section

Methods and any associated references are available in the Supporting Information.

Supporting Information

Supporting Information is available from the Wiley Online Library or from the author.

Acknowledgements

S.L. and M.L. contributed equally to this work. This work was supported by National Key R&D Program of China (2020YFA0710700 and 2017YFA0205600), the National Natural Science Foundation of China (5202500650, 51773191, 51961145109, and 51633008), the Fundamental Research Funds for the Central Universities (WK2070000126), and Outstanding Scholar Program of Bioland Laboratory (Guangzhou Regenerative Medicine and Health Guangdong Laboratory) (2018GZR110102001). All animal experimental procedures were approved by the Institutional Animal Care and Use Committee (IACUC) of the University of Science and Technology of China (USTC). The accreditation number is USTCACUC1701036.

Conflict of Interest

The authors declare no conflict of interest.

Keywords

complement fragments, inflammation treatment, inverted liposomes, neutrophils, voluntary opsonization

Received: September 9, 2020
Revised: November 13, 2020
Published online:

[1] J. W. Yoo, D. J. Irvine, D. E. Discher, S. Mitragotri, *Nat. Rev. Drug Discovery* **2011**, *10*, 521.
[2] A. C. Anselmo, S. Mitragotri, *J. Controlled Release* **2014**, *190*, 531.
[3] a) D. Schmid, C. G. Park, C. A. Hartl, N. Subedi, A. N. Cartwright, R. B. Puerto, Y. Zheng, J. Maiarana, G. J. Freeman, K. W. Wucherpfennig, D. J. Irvine, M. S. Goldberg, *Nat. Commun.* **2017**, *8*, 1747; b) Z. Wang, J. Li, J. Cho, A. B. Malik, *Nat. Nanotechnol.* **2014**, *9*, 204; c) D. Chu, X. Dong, Q. Zhao, J. Gu, Z. Wang, *Adv. Mater.* **2017**, *29*, 1701021; d) J. Hrkach, D. Von Hoff, M. Mukkaram Ali, E. Andrianova, J. Auer, T. Campbell, D. De Witt, M. Figa, M. Figueiredo, A. Horhota, S. Low, K. McDonnell, E. Peeke, B. Retnarajan, A. Sabnis, E. Schnipper, J. J. Song, Y. H. Song, J. Summa, D. Tompsett, G. Troiano, T. Van Geen Hoven, J. Wright, P. LoRusso, P. W. Kantoff, N. H. Bander, C. Sweeney, O. C. Farokhzad, R. Langer, S. Zale, *Sci. Transl. Med.* **2012**, *4*, 128ra39; e) M. E. Davis, J. E. Zuckerman, C. H. Choi, D. Seligson, A. Tolcher, C. A. Alabi, Y. Yen, J. D. Heidel, A. Ribas, *Nature* **2010**, *464*, 1067.
[4] a) S. M. Moghimi, A. C. Hunter, J. C. Murray, *FASEB J.* **2005**, *19*, 311; b) J. Y. Oh, H. S. Kim, L. Palanikumar, E. M. Go, B. Jana, S. A. Park, H. Y. Kim, K. Kim, J. K. Seo, S. K. Kwak, C. Kim, S. Kang, J. H. Ryu, *Nat. Commun.* **2018**, *9*, 4548; c) A. Salvati, A. S. Pitek, M. P. Monopoli, K. Prapainop, F. B. Bombelli, D. R. Hristov, P. M. Kelly, C. Aberg, E. Mahon, K. A. Dawson, *Nat. Nanotechnol.* **2013**, *8*, 137; d) M. P. Monopoli, C. Aberg, A. Salvati, K. A. Dawson, *Nat. Nanotechnol.* **2012**, *7*, 779.
[5] C. D. Walkey, W. C. Chan, *Chem. Soc. Rev.* **2012**, *41*, 2780.
[6] a) M. Lundqvist, J. Stigler, G. Elia, I. Lynch, T. Cedervall, K. A. Dawson, *Proc. Natl. Acad. Sci. USA* **2008**, *105*, 14265; b) S. Tenzer, D. Docter, J. Kuharev, A. Musyanovych, V. Fetz, R. Hecht, F. Schlenk, D. Fischer, K. Kiouptsi, C. Reinhardt, K. Landfester, H. Schild, M. Maskos, S. K. Knauer, R. H. Stauber, *Nat. Nanotechnol.* **2013**, *8*, 772; c) A. E. Nel, L. Madler, D. Velegol, T. Xia, E. M. Hoek, P. Somasundaran, F. Klaessig, V. Castranova, M. Thompson, *Nat. Mater.* **2009**, *8*, 543.
[7] a) H. Otsuka, Y. Nagasaki, K. Kataoka, *Adv. Drug Delivery Rev.* **2003**, *55*, 403; b) Q. Dai, C. Walkey, W. C. Chan, *Angew Chem., Int. Ed. Engl.* **2014**, *53*, 13493.
[8] a) X. Lu, P. Xu, H. M. Ding, Y. S. Yu, D. Huo, Y. Q. Ma, *Nat. Commun.* **2019**, *10*, 4520; b) P. Yousefpour, J. R. McDaniel, V. Prasad, L. Ahn, X. Li, R. Subrahmanyan, I. Weitzhandler, S. Suter, A. Chilkoti, *Nano Lett.* **2018**, *18*, 7784; c) S. Schottler, G. Becker, S. Winzen, T. Steinbach, K. Mohr, K. Landfester, V. Mailander, F. R. Wurm, *Nat. Nanotechnol.* **2016**, *11*, 372; d) K. Saha, M. Rahimi, M. Yazdani, S. T. Kim, D. F. Moyano, S. Hou, R. Das, R. Mout, F. Rezaee, M. Mahmoudi, V. M. Rotello, *ACS Nano* **2016**, *10*, 4421.
[9] a) D. Ricklin, G. Hajishengallis, K. Yang, J. D. Lambris, *Nat. Immunol.* **2010**, *11*, 785; b) M. J. Hickey, P. Kubes, *Nat. Rev. Immunol.* **2009**, *9*, 364; c) S. K. Law, A. W. Dodds, *Protein Sci.* **1997**, *6*, 263.
[10] J. D. Lambris, D. Ricklin, B. V. Geisbrecht, *Nat. Rev. Microbiol.* **2008**, *6*, 132.
[11] M. A. Matthay, R. L. Zemans, G. A. Zimmerman, Y. M. Arabi, J. R. Beitler, A. Mercat, M. Herridge, A. G. Randolph, C. S. Calfee, *Nat. Rev. Dis. Primers* **2019**, *5*, 18.
[12] A. Mantovani, M. A. Cassatella, C. Costantini, S. Jaillon, *Nat. Rev. Immunol.* **2011**, *11*, 519.
[13] F. Wang, J. Liu, *J. Am. Chem. Soc.* **2015**, *137*, 11736.
[14] F. Carlsson, C. Sandin, G. Lindahl, *Mol. Microbiol.* **2005**, *56*, 28.
[15] A. Hidalgo, J. Chang, J. E. Jang, A. J. Peired, E. Y. Chiang, P. S. Frenette, *Nat. Med.* **2009**, *15*, 384.
[16] a) R. Sumagin, H. Prizant, E. Lomakina, R. E. Waugh, I. H. Sarelius, *J. Immunol.* **2010**, *185*, 7057; b) K. Chen, H. Nishi, R. Travers, N. Tsuboi, K. Martinod, D. D. Wagner, R. Stan, K. Croce, T. N. Mayadas, *Blood* **2012**, *120*, 4421.
[17] R. D. Soltis, D. Hasz, M. J. Morris, I. D. Wilson, *Immunology* **1979**, *36*, 37.

[18] S. Zapf, M. Loos, *Immunobiology* **1985**, *170*, 123.
[19] a) F. Chen, G. Wang, J. I. Griffin, B. Brenneman, N. K. Banda, V. M. Holers, D. S. Backos, L. Wu, S. M. Moghimi, D. Simberg, *Nat. Nanotechnol.* **2017**, *12*, 387; b) J. Gbadamosi, A. Hunter, S. Moghimi, *FEBS Lett.* **2002**, *532*, 338.
[20] a) P. K. Hashim, K. Okuro, S. Sasaki, Y. Hoashi, T. Aida, *J. Am. Chem. Soc.* **2015**, *137*, 15608; b) M. Zheng, Y. Liu, Y. Wang, D. Zhang, Y. Zou, W. Ruan, J. Yin, W. Tao, J. B. Park, B. Shi, *Adv. Mater.* **2019**, *31*, 1903277.
[21] S. D. Wright, P. E. Rao, W. C. Van Voorhis, L. S. Craigmyle, K. Iida, M. A. Talle, E. F. Westberg, G. Goldstein, S. C. Silverstein, *Proc. Natl. Acad. Sci. USA* **1983**, *80*, 5699.
[22] J. Bhattacharya, M. A. Matthay, *Annu. Rev. Physiol.* **2013**, *75*, 593.
[23] V. Brinkmann, U. Reichard, C. Goosmann, B. Fauler, Y. Uhlemann, D. S. Weiss, Y. Weinrauch, A. Zychlinsky, *Science* **2004**, *303*, 1532.
[24] W. Gao, Y. Chen, Y. Zhang, Q. Zhang, L. Zhang, *Adv. Drug Delivery Rev.* **2018**, *127*, 46.